

Comparison of short pulse generation schemes for a soft x-ray free electron laser

I. P. S. Martin and R. Bartolini

*Diamond Light Source, Oxfordshire, OX11 0DE, United Kingdom,
and John Adams Institute, University of Oxford, OX1 3RH, United Kingdom*

(Received 5 October 2010; published 7 March 2011)

In this paper we study the performance of two complementary short pulse generation schemes as applied to a soft x-ray free electron laser. The first scheme, recently proposed by Saldin *et al.*, makes use of a laser pulse consisting of only a few optical cycles to give an energy chirp to a short section of an electron bunch and tapers the main radiator undulator in order to compensate the chirped region. The second scheme investigated takes a low-charge, high brightness electron bunch and compresses it to ~ 1 fs in order to operate in the so-called “single-spike” regime. We perform start-to-end simulations of both these schemes, assess the sensitivity of each scheme to realistic jitter sources, and provide a direct comparison of the respective strengths and drawbacks.

DOI: [10.1103/PhysRevSTAB.14.030702](https://doi.org/10.1103/PhysRevSTAB.14.030702)

PACS numbers: 41.60.Cr, 41.75.Fr, 29.27.-a

I. INTRODUCTION

Ultrashort, high brightness x-ray sources would permit considerable advances to be made in many areas of science, such as in single-shot imaging of biological samples and in measuring structural dynamics on subfemtosecond (fs) time scales. Several schemes have recently been proposed for the production of short pulse radiation using high-gain free electron lasers (FELs), the majority of which use a few-cycle optical laser pulse to modulate the electron energy or trajectory in a small section of the bunch. This can be applied as an extension of the enhanced self-amplification of spontaneous emission or echo-enabled harmonic generation based schemes, in which energy modulation is used in combination with magnetic chicane to enhance the local current density [1–3]. Other schemes selectively amplify the radiation emitted by the maximum energy-offset portion of the bunch in several stages [4,5], or alternatively the radiation from this portion can be selected after saturation in a single stage undulator using a monochromator [6]. One proposal uses a modulating laser to give a large energy chirp to the electron bunch and compensates this region by tapering the main undulator [7,8]. Another method applies an angular trajectory modulation to a short section of the electron bunch and arranges for this to be the new reference trajectory in the main undulator in order to suppress the gain from the remainder of the bunch through slippage effects [9]. One key aspect of all these schemes is that the initial modulating laser pulse can be used as a synchronization trigger, a key requirement for pump-probe experiments.

Aside from these laser-based schemes, other techniques which have been proposed include spoiling the emittance

of all but a small section of the electron bunch by passing it through a slotted foil [10], passing an ultrashort, low-charge electron bunch through the FEL in order to operate in the single-spike regime [11], or using a monochromator to select a short pulse from the radiation emitted by an energy-chirped electron beam to use as a seed for a second stage undulator [12]. Alternatively, the pulse emitted by an energy-chirped electron bunch can be used directly after optical compression [13].

Experimental evidence for these schemes is limited. None of the laser slicing methods have been demonstrated to date. Single-spike operation on longer wavelength FELs has been performed [14], as has a low-charge mode for the Linac Coherent Light Source (LCLS) [15,16]. Operation of the LCLS with a slotted foil is also showing promising first signs [16]. As a result of this paucity of evidence, in-depth numerical simulations of such schemes are still required.

In this paper we investigate the performance of two of these schemes for a soft x-ray FEL, taking the UK’s New Light Source Project (NLS) [17] as a practical example. The science case for this project suggests an ideal short pulse would consist of a single, isolated radiation pulse of <1 fs synchronized to an external trigger. None of the schemes mentioned above can meet this demand in entirety, and so consideration must be given as to which schemes would most closely meet these requirements.

Considering the predicted achievable performance, additional hardware required, and operational complexity, a comparison of the above schemes suggested the tapered undulator scheme and single-spike operation for further study. While the majority of the laser slicing schemes can produce synchronized, short radiation pulses, the background pedestal can still form a significant fraction of the total pulse energy. The tapered undulator scheme suppresses this background, and delivers short pulses with minimal additional infrastructure to the baseline facility. Such an undulator taper can also be used to enhance other,

Published by American Physical Society under the terms of the Creative Commons Attribution 3.0 License. Further distribution of this work must maintain attribution to the author(s) and the published article’s title, journal citation, and DOI.

more complex, short pulse schemes [18]. Single-spike operation has effectively no radiation background and can be implemented with no additional hardware, also making it an attractive proposition despite the lack of tight synchronization control. We build on previous studies of these schemes [7,8,19] by performing full start-to-end simulations, assessing the sensitivity of each scheme to realistic jitter sources and providing further understanding of their respective performances and further insight in the complicated dynamics which governs the interaction of the electron beam with the FEL electromagnetic field.

II. ENERGY CHIRP WITH TAPERED UNDULATORS

The short pulse scheme proposed by Saldin *et al.* [7] uses a laser pulse consisting of only a few optical cycles to modulate the electron bunch energy at the laser wavelength, and compensates for the resulting time-dependent energy chirp by tapering the undulator gap in the main radiator. Since only a small part of the electron bunch will have the required value of energy chirp to be matched to the undulator taper, only this section of the bunch will experience exponential gain. The remainder of the bunch will suffer from strong gain degradation, leading to an excellent contrast ratio between the short pulse radiation and radiation background.

A. Parametrization of tapered undulator scheme

The required undulator taper to compensate a given energy chirp was calculated by Saldin *et al.* [7] to be

$$\frac{1}{H_u} \frac{dH_u}{dz} = -\frac{1}{2} \frac{(1+K^2)^2}{K^2} \frac{1}{\gamma_0} \frac{d\gamma}{cdt}, \quad (1)$$

where z is the distance through the undulator, H_u is the magnetic field of the undulator, K is the undulator parameter, and γ_0 is the relativistic parameter for the reference particle.

The underlying physics of the scheme can be understood as follows. If we consider the radiation emitted by an electron towards the back of the bunch, this radiation field will gradually slip forwards to particles with a different energy. In order for the resonant wavelength to remain unchanged and thus continued strong radiation gain, the K parameter must be adjusted accordingly. One side effect of this scheme is that the radiation pulse also acquires a frequency chirp.

B. Simulation details

The energy modulator consists of a two-period planar undulator with $\lambda_m = 140$ mm, resonant at the slicing laser wavelength. The main radiator consists of APPLE-II helical undulator modules with $\lambda_u = 32.2$ mm interleaved in a focusing-defocusing (FODO) lattice, and is set to be resonant at $\lambda_0 = 1.24$ nm in the first module. The main components of the scheme are shown in Fig. 1.

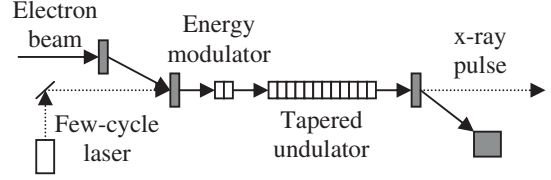


FIG. 1. Main components of the tapered undulator scheme.

For the studies of this scheme we use the electron bunch optimized for standard NLS operation [17], namely, a 2.25 GeV, 0.2 nC electron bunch with 0.3 mm mrad normalized slice emittance, 160 keV energy spread, and 1120 A peak current. This bunch has a ~ 50 fs long region with constant slice parameters, large enough to accommodate the expected jitter between slicing laser and electron bunch arrival times. The start-to-end simulations are carried out using the codes ASTRA [20], ELEGANT [21], and GENESIS [22]. The effect of the modulating laser is calculated numerically in ELEGANT, with the phase of the laser set to $\pi/2$ (sine mode) in order to give maximum energy chirp to the center of the distribution (see Fig. 2). In analogy to single-spike operation [19], for the FEL pulse to consist of a single SASE radiation spike and to reach saturation, the portion of the bunch with linear energy chirp must have a length matched to the cooperation length of the FEL; i.e.

$$L_{\text{linear chirp}} \cong 2\pi L_c, \quad (2)$$

where the cooperation length (L_c) is defined as

$$L_c = \frac{\lambda_0}{4\pi\sqrt{3}\rho} \quad (3)$$

and ρ is the Pierce parameter. For the above electron bunch parameters, $\rho = 1.2 \times 10^{-3}$ and so the optimal linear energy chirp duration is estimated to be ~ 1 fs.

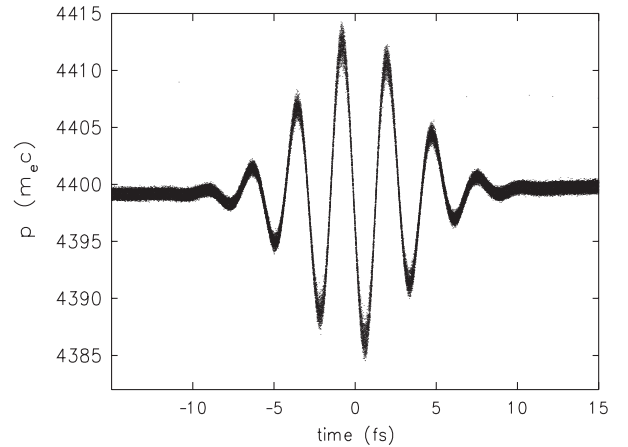


FIG. 2. Energy modulation given to the electron bunch by the combined undulator-laser interaction. An 800 nm, 5 fs FWHM, 0.4 mJ laser pulse was assumed.

C. Baseline performance

An extensive campaign of numerical simulations has allowed the identification of how each of the modulating laser parameters affects the final FEL pulse qualities [23]. Varying the laser wavelength was found to have the strongest effect. If it is too long then the FEL pulse will also be long, defeating the main goal of the scheme and potentially allowing more than one SASE radiation spike to develop. If it is too short then the FEL pulse saturates at a lower peak power than would otherwise be the case, and the pulse does not develop into a clean single spike. Altering the laser pulse duration changes the relative amplitude of the satellite peaks to the central one; the longer the laser pulse the larger and more numerous the satellite peaks become. In the limit of a continuous modulating laser, a train of equispaced short radiation pulses will be produced. Increasing the energy of the laser pulse leads to a larger energy chirp which in turn requires a stronger undulator taper to compensate. This has the effect of improving the contrast ratio between the main peak and the background radiation (and also to the satellite peaks). The FEL pulse width is also marginally shortened and the linewidth broadened. However, this comes at the expense of a decrease in saturation power. It was noted in [7] that a mild positive energy chirp is beneficial to the SASE process, and that decreasing the undulator taper can lead to higher power at saturation. The down side of reducing the undulator taper is that the match to the rest of the bunch is improved and so the contrast ratio is reduced.

From this study, two possible operating scenarios were identified. The first option uses an 800 nm, 5 fs FWHM laser with 0.4 mJ pulse energy, with the optimum taper for the radiator undulator found to be 90% of the value given by Eq. (1). These laser parameters appear to be feasible with current technology [24–26]; however, at ~ 0.4 fs the length of linear chirp is too short when compared to the cooperation length of the FEL. The alternative solution is to use a 1600 nm, 0.4 mJ, 10 fs FWHM laser as this gives a better match to the cooperation length constraint (2). However, these laser parameters are yet to be demonstrated experimentally. Figure 3 shows the growth in peak power along the undulator for these two options, calculated as mean values over 100 different shot-noise seeds. Figure 4 shows the corresponding averaged temporal profiles at saturation, taken to occur at 34.4 m (25.1 m of active undulator length). Pulse properties are summarized in Table II.

The effect of increasing the slicing laser wavelength from 800 to 1600 nm are clear from Fig. 4; there is a fourfold increase in saturation power which comes at the expense of an increase in pulse duration. The temporal profile and spectrum for the 800 nm laser are shown in Figs. 5 and 6 respectively for a single-shot-noise seed, and contain the salient features of all the pulse profiles obtained using this scheme. The radiation can be seen to consist of a dominant central radiation peak, with two, smaller satellite

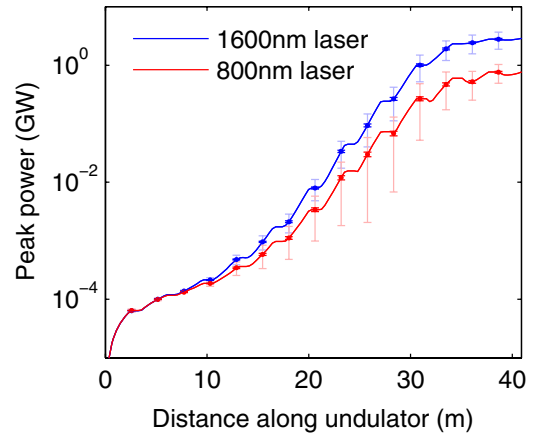


FIG. 3. Power growth along the undulator for the 1600 and 800 nm slicing laser wavelength options. Bold error bars show the error on the mean value; faint error bars show standard deviation over 100 shot-noise seeds.

peaks located at ± 2.7 fs with respect to the central peak (i.e. separated by the laser period). However, for the case of an 800 nm modulating laser, neither the central peak nor the satellite peaks are clean single spikes, but rather they consist of a series of subspikes. Each subspike is predominantly the emission from the chirped region of the electron pulse within a single undulator module, and is separated in time from the previous one by the slippage that occurs between each module. This behavior is a direct result of having too short a region of linear energy chirp compared to the cooperation length of the FEL, and is not observed when using a modulating laser wavelength of 1600 nm (where a better match is achieved).

The spectrum at saturation shown in Fig. 6 shows some fringing due to interference between the radiation in the main peak and that emitted in the satellite peaks. To remove these fringes from the spectrum, the modulating laser should consist of a true single cycle, or the amplitude

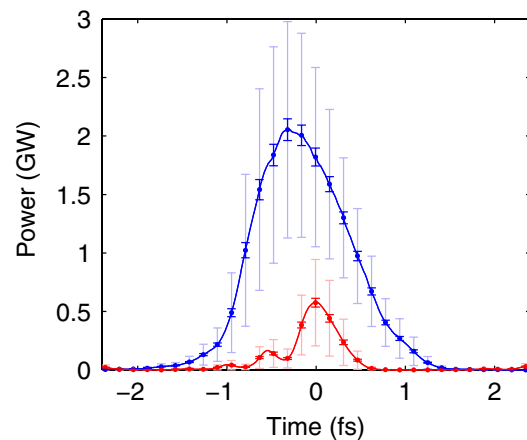


FIG. 4. Power at saturation for the 1600 and 800 nm slicing laser wavelength options. Bold error bars show the error on the mean value; faint error bars show standard deviation over 100 shot-noise seeds.

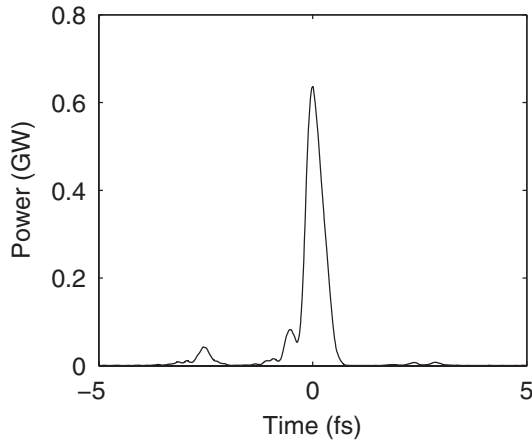


FIG. 5. Temporal profile of a single FEL radiation pulse at 34.4 m for the case of an 800 nm modulating laser. The radiation consists of a dominant central peak surrounded by two, smaller peaks separated by the laser period.

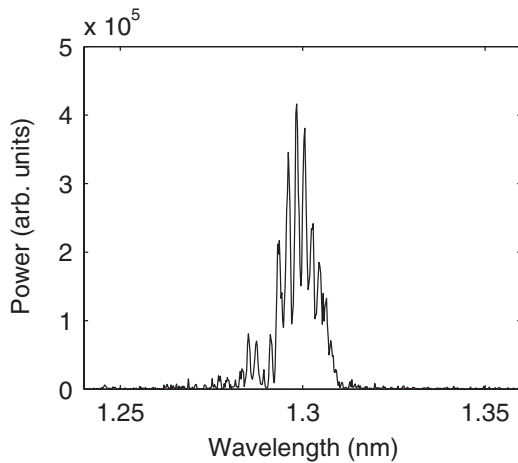


FIG. 6. Spectrum of a single FEL radiation pulse at 34.4 m for the case of an 800 nm modulating laser. The fringing in the spectrum is due to interference between the radiation emitted by the central and satellite peaks.

of the satellite FEL radiation peaks should be negligibly small.

D. Manipulation of FEL pulse

To investigate the pulse properties in more depth, we take a Wigner transform of the radiation field integrated across a $1.4 \text{ mm} \times 1.4 \text{ mm}$ aperture at the observation point (34.4 m) for the 800 nm laser option (see Fig. 7) [8]. Because of the taper in undulator gap, the central wavelength shifts from 1.24 nm after the first undulator module to 1.30 nm at saturation, both for the central and satellite radiation peaks. This suggests that the unwanted radiation emitted upstream of the final undulator module can be filtered out with a relatively wide acceptance monochromator, restoring the central radiation peak to a clean single spike. In addition to this, there is a frequency chirp

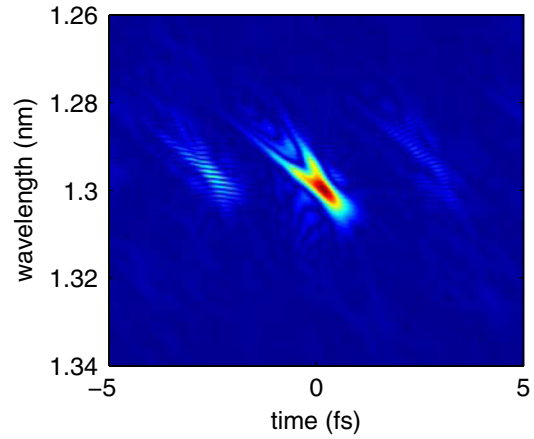


FIG. 7. Wigner transform of the radiation field at 34.4 m for the 800 nm modulating laser case. The radiation emitted at earlier times is clearly visible at shorter wavelengths.

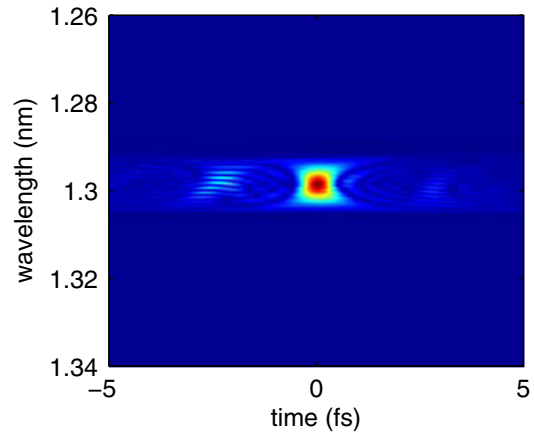


FIG. 8. Wigner transform of the radiation field at 34.4 m for the 800 nm modulating laser case. The pulse has been filtered and compressed to maximize the peak power and remove radiation emitted upstream.

of $\sim 0.01 \text{ nm/fs}$ across the radiation pulse. As noted in [8], this can be used to further compress the radiation pulse using a grating compressor [13]. The Wigner transform for the radiation pulse after such a process is shown in Fig. 8. The filter used was centered on the peak wavelength with a pass bandwidth of 1×10^{-2} . The filtering and compression of the radiation pulse can also be carried out after the nominal saturation point thanks to the wavelength shift after each undulator, allowing a greater fraction of pulses to reach saturation. This is demonstrated in Fig. 9, in which the average over 100 unmodified radiation pulses at 37.7 m is compared to that of 100 pulses which have been filtered and compressed. We also note that, although the cooperation length places a lower limit on the FEL pulse duration under normal circumstances, filtering and compressing the radiation has effectively side-stepped this constraint and led to a reduction in pulse length to 0.5 fs compared to the $\sim 1 \text{ fs}$ predicted from the cooperation length. In addition,

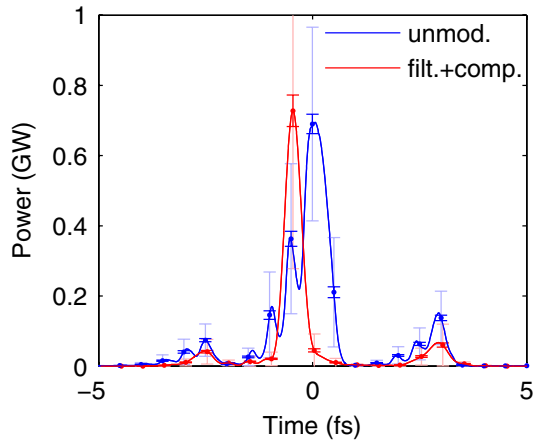


FIG. 9. Comparison of unmodified to filtered and compressed radiation pulses at 37.7 m averaged over 100 shot-noise seeds.

the pulse duration calculated from the integrated field is the same as the value calculated from the on-axis, far field data, demonstrating the short pulse is preserved over a large area. The main properties of the 100 filtered and compressed pulses are summarized in Table II.

TABLE I. Jitter sources included in the start-to-end tracking simulations (rms values).

Source	Value
Solenoid field	0.01%
Gun phase	0.1%
Gun voltage	0.1%
Charge	1%
Gun laser spot offset	0.025 mm
Linac cavity phase	0.01%
Linac cavity relative voltage	10^{-4}
3rd harmonic cavity phase	0.03%
3rd harmonic cavity relative voltage	3×10^{-4}
Bunch compressor power supply	10^{-5}
Modulating laser phase	0.2 rad

TABLE II. Table of FEL pulse properties taken as averages over 100 seeds.

	Tapered undulator scheme			Single spike		
	1600 nm laser	800 nm laser	800 nm laser (filtered + compressed)	800 nm laser (jittered)	2 pC	2 pC (jittered)
Distance in undulator (m)	34.4 m	34.4 m	37.7 m	34.4 m	17.7 m	17.7 m
Peak power (GW)	2.31 ± 0.08	0.59 ± 0.04	0.76 ± 0.05	0.66 ± 0.04	1.71 ± 0.10	2.16 ± 0.16
Energy in main peak (μJ)	2.36 ± 0.10	0.35 ± 0.03	0.37 ± 0.02	0.42 ± 0.03	0.81 ± 0.05	1.01 ± 0.07
Pulse length, FWHM (fs)	1.07 ± 0.02	0.45 ± 0.01	0.49 ± 0.01	0.52 ± 0.02	0.44 ± 0.01	0.46 ± 0.02
Linewidth (pm)	4.65 ± 0.17	8.8 ± 0.2	9.0 ± 0.2	8.9 ± 0.3	6.3 ± 0.1	5.8 ± 0.1
Time bandwidth	0.96 ± 0.04	0.78 ± 0.03	0.85 ± 0.03	0.91 ± 0.05	0.53 ± 0.02	0.50 ± 0.01
Radiation beam size (μm)	38 ± 0.3	38 ± 0.5	35 ± 0.3	44 ± 2	29 ± 0.3	29 ± 0.3
Arrival time jitter (fs)	0.23	0.06	0.13	0.11	0.09	12.68
Average background power (MW)	7.5 ± 0.3	0.7 ± 0.1	0.1 ± 0.1	1.9 ± 0.1

E. Sensitivity to jitter sources

In the previous sections a constant, idealized electron bunch distribution was assumed. A real accelerator suffers from shot-to-shot fluctuations on top of the SASE variability, and any practical short pulse generation scheme must be able to cope with these changes. To investigate the sensitivity of the proposed scheme to these jitter sources, 100 start-to-end simulations were carried out after applying the errors detailed in Table I. These errors were varied in Gaussian distributions truncated at 3 sigma, and the values were arrived at considering operational experience at FLASH (or modest improvement on these values) [27,28]. The bunch compressors were assumed to be powered in series, and each rf cavity in the cryomodules was modeled as being fed independently.

The results of these simulations are summarized in Table II. While there is a small degradation in most parameters when jitter sources are included in the simulations, the peak power at saturation is found to be largely unaffected and is rather dominated by the intrinsic SASE variability.

III. SINGLE-SPIKE OPERATION

As an alternative to the tapered undulator scheme, we have also investigated the performance of low-charge, single-spike operation. Whereas in the tapered undulator scheme only the length of linear energy chirp needs to be matched to the cooperation length of the FEL, in this scheme it is the entire electron bunch length L_e that is tailored to satisfy the condition

$$L_e \cong 2\pi L_c. \quad (4)$$

In the case of the NLS, this means reducing the electron bunch length to $\lesssim 1$ fs. If this condition can be met, the FEL output will consist of a single SASE radiation spike with good transverse and temporal coherence [29]. This level of bunch compression is best achieved at very low bunch charges (below 10 pC), when the impacts of collective effects are much reduced and a very high beam

quality can be maintained from the rf gun, through the linac to the entrance of the undulators.

The main benefits of this mode of operation are simplicity of implementation, the lack of background radiation pedestal, and the high-degree of longitudinal coherence which are produced. However, because the FEL process is initiated by the SASE mechanism it is expected to suffer from large shot-to-shot fluctuations in the output power, and since the FEL output is not synchronized to an external laser, any jitter in the arrival time of the electron beam will be transferred directly to timing jitter in the FEL output. One further drawback with this mode of operation is that machine diagnostics are very difficult to operate at such low bunch charges.

A. Start-to-end simulations

The performance of the scheme has been studied with start-to-end simulations using a combination of ASTRA, ELEGANT, and GENESIS. The gun, linac, and FEL models used were similar to those used for the tapered undulator scheme, with the exception that the energy modulator was removed. Undulator lengths were also slightly different at 3.83 m compared to 2.51 m, reflecting the facility layout at an early design stage. The gun charge was reduced to 2 pC and the linac working point reoptimized using the maximum peak current and electron bunch length as target parameters. In doing this limits were placed on the maximum chicane magnet bend angles and accelerating cavity phases in order to keep timing jitter as low as possible and to minimize the final energy chirp on the electron bunch. The compression in the main linac takes the electron bunch from a peak current of 0.55 A and 3.8 ps FWHM at the exit of the injector to a peak current of 1.9 kA and 0.8 fs FWHM at the undulator entrance. The normalized slice emittance and energy spread at the undulator entrance are 0.065 mm mrad and 470 keV, respectively, highlighting the improvement in beam brightness that is possible when the bunch charge is reduced. While these values at first sight appear aggressive, they are consistent with values found in other studies and with operational experience at LCLS during low-charge operation [15,19].

Simulations using the final electron bunch distribution were carried out for 100 different shot-noise seeds using GENESIS in time-dependent mode. The average power growth along the undulator is shown in Fig. 10. If saturation is taken to occur at 22.2 m, the x-ray temporal profiles are frequently found to be distorted or to have more than one radiation spike in the output. However, taking the radiation output one undulator module earlier at 17.7 m, the pulse profiles are found to be much cleaner, consisting of a single radiation spike and to have a smaller pulse length (albeit with lower peak power). The average of the x-ray pulse profiles at 17.7 m is shown in Fig. 11. Note that 17.7 m corresponds to 15.3 m of active undulator length, compared to 25.1 m in the tapered undulator scheme; a direct benefit of the substantial increase in beam brightness

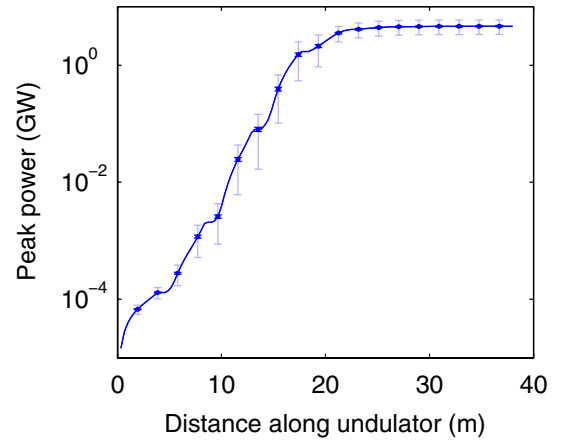


FIG. 10. Mean power growth along the undulator for 100 shot-noise seeds. Bold error bars show the error on the mean value; faint error bars show standard deviation.

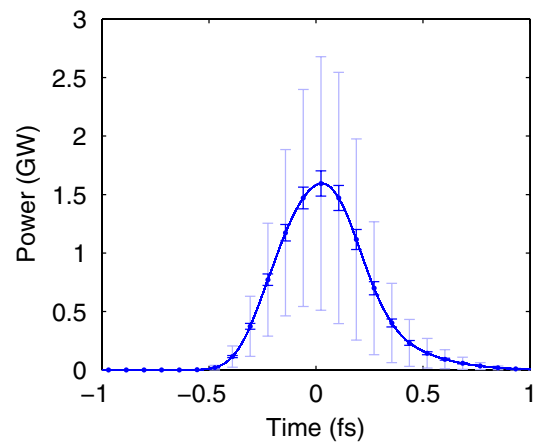


FIG. 11. Mean power at 17.7 m calculated over 100 shot-noise seeds. Bold error bars show the error on the mean value; faint error bars show standard deviation.

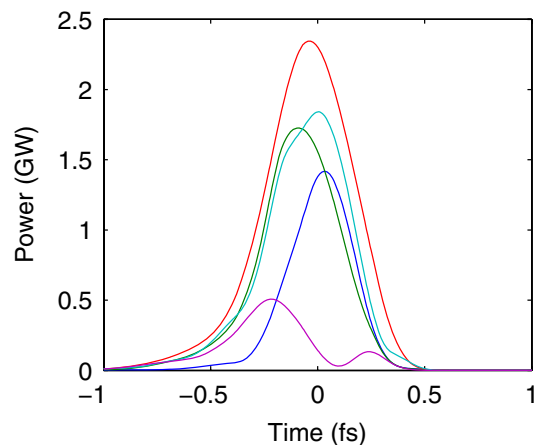


FIG. 12. Selection of FEL pulse temporal profiles at 17.7 m calculated using different shot-noise seeds.

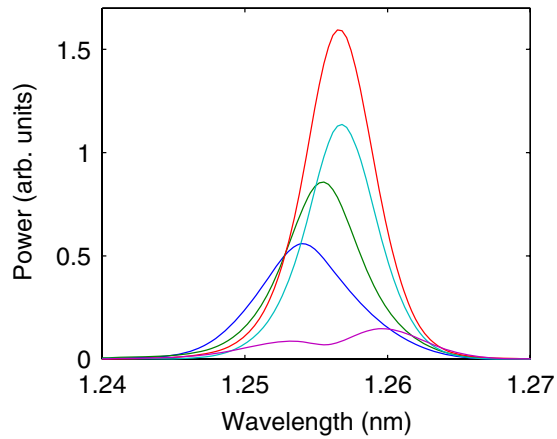


FIG. 13. Selection of FEL pulse spectra at 17.7 m calculated using different shot-noise seeds.

for low-charge operation. The pulse properties averaged over 100 shot-noise seeds are summarized in Table II.

A selection of the pulse profiles at saturation is shown in Fig. 12, and the corresponding spectral profiles are shown

in Fig. 13. From this it is clear that, while the vast majority of seeds produced clean single spikes, occasional seeds produce a somewhat lower power with two spikes appearing in both the temporal and spectral profiles.

Operating at maximum compression leaves the electron bunch with a relatively high energy spread, predominately due to the chirp given to the beam during acceleration and compression. This can be mitigated by running slightly above or below maximum compression at the expense of lengthening the electron bunch and lowering the peak current. However, since the cooperation length is also increased, the bunch length constraint given by Eq. (4) is also relaxed.

A plot showing how the electron bunch length varies as a function of bunch compressor strength is given in Fig. 14. For each electron bunch length, GENESIS simulations were carried out for 40 different shot-noise seeds, and FEL pulse energy, length and linewidths at saturation were calculated (also shown in Fig. 14). An examination of the resulting radiation pulse temporal profiles showed that, as expected, the number of seeds giving rise to more than one radiation

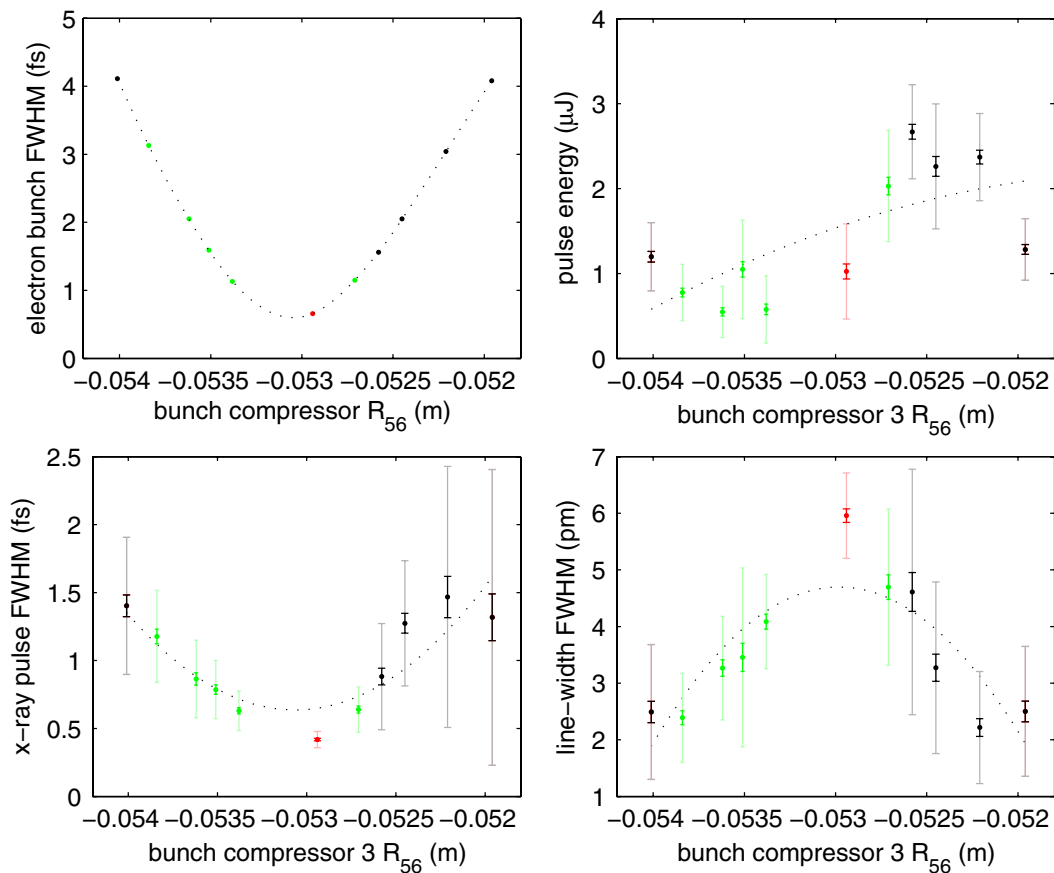


FIG. 14. Electron bunch and x-ray pulse properties as a function of bunch compressor strength taken as average values over 40 shot-noise seeds. Shown are plots of electron bunch length (top left), pulse energy (top right), x-ray pulse length (bottom left), and pulse linewidth (bottom right). Data for bunch lengths which produce single-spike behavior on the majority of seeds has been highlighted in green, and data for maximum compression in red. Bold error bars show the error on the mean values, and faint error bars show standard deviation over 40 shot-noise seeds.

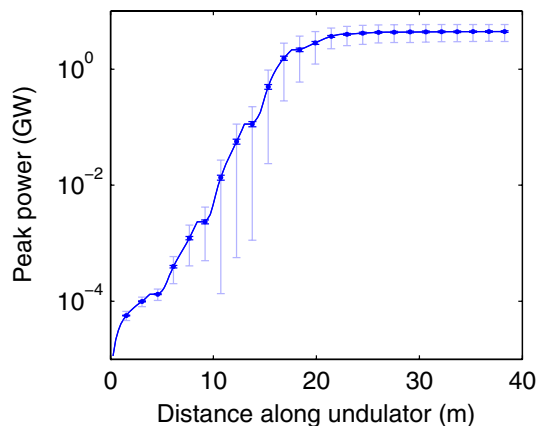


FIG. 15. Mean power growth along the undulator for 100 different random seeds. Calculations are performed including realistic gun and linac errors. Bold error bars show the error on the mean value; faint error bars show standard deviation.

spike was found to increase as the length of the electron bunch increased. Only the bunch lengths between 1 fs undercompressed to 3 fs overcompressed showed single-spike behavior in the output.

B. Sensitivity to jitter sources

The sensitivity of the FEL output for single-spike operation on realistic jitter sources was again tested by adding random, Gaussian distributed errors to various components in the gun and main linac, the values for which are listed in Table I. Start-to-end simulations were performed for 100 different error seeds, with the linac set to operate at maximum bunch compression.

The resulting average power growth along the undulator is shown in Fig. 15, and the x-ray pulse profiles as a function of time are shown in Fig. 16. The pulse parameters are summarized in Table II. The introduction of gun and linac errors has led to a modest increase in the majority of

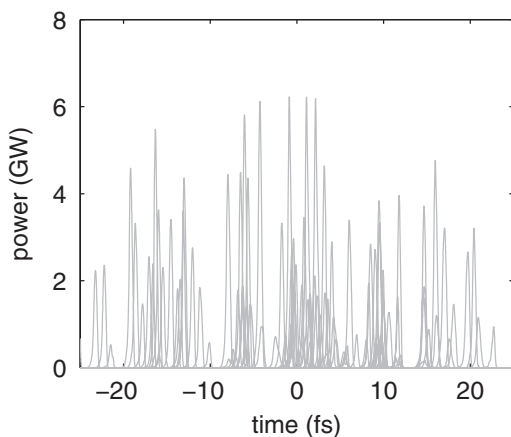


FIG. 16. Power at saturation for 100 different random seeds. Calculations are performed including realistic gun and linac errors.

parameters, but as with the tapered undulator scheme there is no significant change in the peak power at saturation, with the intrinsic SASE variability dominating. The most significant effect of the gun and linac errors is in the increase in rms arrival time jitter from 0.1 to 12.7 fs.

IV. CONCLUSIONS

We have investigated two complementary short pulse generation schemes applied to a soft x-ray FEL. While the tapered undulator scheme has the potential drawback of having a SASE radiation background from the main bunch, the undulator taper means the average background power is 3 orders of magnitude below the peak power of the central spike. With careful selection of the operating laser and undulator taper parameters, the amplitude of the satellite peaks can also be reduced to well below that of the central peak. For the case of an 800 nm modulating laser, we have also demonstrated that with filtering and compression of the FEL pulse after saturation it is possible to reduce the pulse duration to below the one implied by the cooperation length.

For single-spike operation we have found that, as expected, the shortest FEL pulse is produced at maximum compression for the electron bunch. However, operating at slight undercompression has the advantage of a moderate increase in the total energy per pulse. The potential drawback of this scheme is the lack of tight synchronization control, but this may be mitigated with the use of sophisticated time-stamping techniques [30], or by using the same electron bunch to generate both the pump and probe radiation pulses directly [31].

Both schemes are able to produce sub-fs, GW-level pulses with a high degree of longitudinal coherence, even after taking realistic jitter sources into account. Time-bandwidth products for both schemes are on average below 1, and the values for single-spike operation are only marginally above the 0.44 value found for Gaussian distributions.

These schemes hold great promise for the production of ultrashort radiation pulses, providing the necessary tools for the development of ultrafast science with soft x-ray FELs.

ACKNOWLEDGMENTS

The authors would like to thank J.-H. Han for providing the electron gun distributions used for this study and J. Rowland for developing the software used for the jitter studies. Many useful discussions with G. Hirst, R. Walker, and members of the NLS physics and parameters working group are also gratefully acknowledged.

-
- [1] A. Zholents, *Phys. Rev. ST Accel. Beams* **8**, 040701 (2005).
 - [2] A. Zholents and G. Penn, *Phys. Rev. ST Accel. Beams* **8**, 050704 (2005).

- [3] D. Xiang, Z. Huang, and G. Stupakov, *Phys. Rev. ST Accel. Beams* **12**, 060701 (2009).
- [4] E. Saldin, E. Schneidmiller, and M. Yurkov, *Opt. Commun.* **239**, 161 (2004).
- [5] A. Zholents and W. Fawley, *Phys. Rev. Lett.* **92**, 224801 (2004).
- [6] E. Saldin, E. Schneidmiller, and M. Yurkov, *Opt. Commun.* **237**, 153 (2004).
- [7] E. Saldin, E. Schneidmiller, and M. Yurkov, *Phys. Rev. ST Accel. Beams* **9**, 050702 (2006).
- [8] W. Fawley, *Nucl. Instrum. Methods Phys. Res., Sect. A* **593**, 111 (2008).
- [9] A. Zholents and M. S. Zolotarev, *New J. Phys.* **10**, 025005 (2008).
- [10] P. Emma *et al.*, *Phys. Rev. Lett.* **92**, 074801 (2004).
- [11] R. Bonifacio, B. McNeil, A. Paes, L. de Salvo, and R. Galvão, *Int. J. Infrared Millim. Waves* **28**, 699 (2007).
- [12] C. Schroeder, C. Pellegrini, S. Reiche, J. Arthur, and P. Emma, *Nucl. Instrum. Methods Phys. Res., Sect. A* **483**, 89 (2002).
- [13] C. Pellegrini, *Nucl. Instrum. Methods Phys. Res., Sect. A* **445**, 124 (2000).
- [14] L. Giannessi *et al.*, in Proceedings of FEL 2010 (2010), <http://srv-fel-0.maxlab.lu.se/TOC/MOOA14.pdf>.
- [15] Y. Ding *et al.*, *Phys. Rev. Lett.* **102**, 254801 (2009).
- [16] J. Frisch *et al.*, Report No. SLAC-PUB-14251, 2010.
- [17] NLS Project: Conceptual Design Report (2010).
- [18] Y. Ding, Z. Huang, D. Ratner, P. Bucksbaum, and H. Merdji, *Phys. Rev. ST Accel. Beams* **12**, 060703 (2009).
- [19] S. Reiche, P. Musumeci, C. Pellegrini, and J.B. Rosenzweig, *Nucl. Instrum. Methods Phys. Res., Sect. A* **593**, 45 (2008).
- [20] K. Flottmann, <http://www.desy.de/~mpyflo>.
- [21] M. Borland, APS Report No. LS-287.
- [22] S. Reiche, *Nucl. Instrum. Methods Phys. Res., Sect. A* **429**, 243 (1999).
- [23] I. Martin and R. Bartolini, in Proceedings of FEL2010 (2010), <http://srv-fel-0.maxlab.lu.se/TOC/WEPA01.pdf>.
- [24] A. Cavalieri *et al.*, *New J. Phys.* **9**, 242 (2007).
- [25] J. Rauschenberger *et al.*, *Laser Phys. Lett.* **3**, 37 (2006).
- [26] A. Verhoef *et al.*, *Appl. Phys. B* **82**, 513 (2006).
- [27] H. Schlarb *et al.*, in Proceedings of DIPAC 2007 (2007), p. 307, <http://accelconf.web.cern.ch/AccelConf/d07/papers/WEPC01.pdf>.
- [28] S. Schreiber *et al.*, in Proceedings of EPAC 2008 (2008), p. 133, <http://accelconf.web.cern.ch/AccelConf/e08/papers/MOPC030.pdf>.
- [29] R. Bonifacio *et al.*, *Phys. Rev. Lett.* **73**, 70 (1994).
- [30] E. Saldin, E. Schneidmiller, and M. Yurkov, *Phys. Rev. ST Accel. Beams* **13**, 030701 (2010).
- [31] B. Faatz *et al.*, *Nucl. Instrum. Methods Phys. Res., Sect. A* **475**, 363 (2001).